UNI ERSITY OF READING

Analysis and Computation of Steady Open Channel Flow using a Singular Perturbation Problem [†]

I MacDonald, M J Baine and N K Nichol

Numerical Analysis Report **7/ 4**

Department of Mathematics
University of Reading
P Box 220
Reading
RG6 2AX
United Kingdom

[†] This work forms part of the research programme of the Institute for Computational Fluid Dynamics at Oxford and Reading and was supported by the SERC and HR Wallingford Ltd.

Abstract

In this work we consider steady state solutions of the Saint-Venant equations. We approach these solutions by adding a small artificial viscosity term to the steady Saint-Venant equations and then considering the limit as this term goes to zero. We show that for a uniform rectangular channel, and under certain assumptions, that this limiting process gives a unique physical solution to the problem. We show that in these cases the limiting process also gives us a well-behaved numerical scheme for the computation of this solution. Numerical results are given for a set of test problems and compared with the analytic solutions.

Contents

1 Background

1.1 The Steady Saint-Venant Equation

The flow of water in an open channel can be modelled by the Saint-Venant equations. This model approximates the actual flow by a one-dimensional flow. A system of two conservation laws is derived using principles of mass and momentum balance. For these equations to be valid various assumptions about the channel and the flow are required, but we will not consider the question of validity here. A derivation of the Saint-Venant equations can be found in Cunge *et al*[3].

In this work we investigate steady state solutions of the Saint-Venant equations and in particular numerical methods for their computation. By steady state solutions we mean solutions that are constant in time. We are interested in such solutions from a practical point of view since steady flow often occurs in nature.

A steady form of the Saint-Venant equations, which we refer to as the steady Saint-Venant equation, is found by assuming that all the variables are time invariant in the unsteady equations. We state the steady Saint-Venant equation below.

Let the x-axis be horizontal and in a direction along the channel length. Figure 1 shows a typical channel cross-section normal to the x-axis. Let $y(x)$ be the depth of the flow at this section, which is the height of the free surface (assumed to be a horizontal line) above the lowest point in the section, and $Q(x)$ be the discharge, the rate at which a volume of water flows through the section. We also need the following functions which come from the shape of the section:

$\sigma(x,\eta)$: Width of the section at height η above the lowest point in the section.

$A(x,y)$: Cross-sectional area of the flow passing through the section, for depth y, and given by

$$A(x,y) = \int_0^y \sigma(x,\eta)d\eta. \tag{1.1}$$

$P(x,y)$: Perimeter length of the flow in contact with the channel.

Figure 2 shows a side view of the channel with the channel bottom a distance $z(x)$ below the x-axis. Let $S_0(x) = \frac{dz}{dx}$ be the slope of the channel bed. The height of the free surface above the x-axis is given by $y(x) - z(x)$.

The steady form of the conservation of mass equation is then

$$Q(x_1) = Q(x_2), \tag{1.2}$$

for any x_1, x_2 along the channel. This equation is trivial and tells us that the discharge is constant throughout the length of the channel. In future we will take this constant value as a known parameter Q.

The corresponding "conservation of momentum" equation is

$$F(x_2, y(x_2)) - F(x_1, y(x_1)) = \int_{x_1}^{x_2} d(x, y(x))dx, \tag{1.3}$$

for any x_1, x_2 along the channel. Here F is a quantity called the Specific Force given by

$$F(x,y) = \frac{Q^2}{A(x,y)} + g\int_0^y (y-\eta)\sigma(x,\eta)d\eta, \tag{1.4}$$

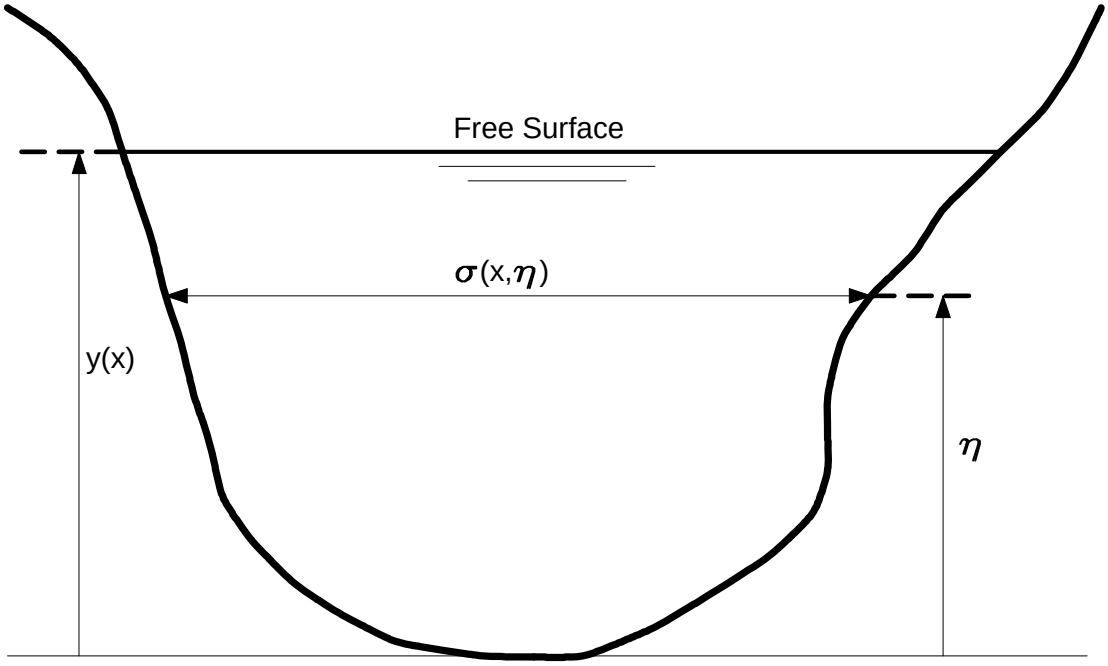

Figure 1: Cross-section of channel, normal to x-axis

where g is the acceleration due to gravity. This quantity has units of force per unit mass and has two components. The first term is the momentum flux due to the flow of water and the second is due to hydrostatic pressure forces. The source term $d(x, y)$ is given by

$$d(x,y) = gA(x,y)\left(S_0(x) - S_f(x,y)\right) + g\int_0^y (y-\eta)\frac{\partial}{\partial x}\sigma(x,\eta)d\eta. \tag{1.5}$$

The friction slope, S_f, models the effects of channel friction and turbulence. There are several common forms for this term; we shall use the form due to Manning (see Chow [2]), which is given by

$$S_f(x,y) = Q|Q|n^2\frac{[P(x,y)]^{4/3}}{[A(x,y)]^{10/3}}, \tag{1.6}$$

where n is the Manning roughness coefficient which controls the roughness of the channel.

From now on we shall make the assumption that $Q > 0$ without loss of generality, since if $Q < 0$ we can simply reverse the x-direction. Also the case $Q = 0$ is trivial.

At any point along the channel where the depth y behaves smoothly, and as long as the channel geometry is smooth enough, we can take the limit as $x_1 \to x_2 \to x$ in equation (1.3) to obtain the differential equation

$$\frac{d}{dx}F(x,y) = d(x,y). \tag{1.7}$$

It is clear that if a stretch of channel has a discontinuous flow then this differential equation does not describe the flow globally. The integral form (equation 1.3),

1.2 Solution Profile for a Rectangular Channel

Although the solutions to equation (1.9) for a general channel shape are difficult to obtain, for certain channel geometries we can get a very good idea of how the solutions behave. Suppose that we restrict attention to a uniform rectangular channel given by $\sigma(x,\eta) = B$, $A(x,y) = By$, $P(x,y) = 2y + B$, where $B > 0$ is a constant. We will also assume that the bed slope, S_0, is constant. Equation (1.9) then becomes the autonomous equation

$$\frac{dy}{dx} = \frac{\Gamma_1(y)}{\Gamma_2(y)}, \tag{1.11}$$

where

$$\Gamma_1(y) = S_0 - Q^2 n^2 \frac{(2y+B)^{4/3}}{(By)^{10}}$$

The main question now is how do we determine the relative positions of y_n and y_c? It turns out that this can be done by classifying the slope, S_0, as follows (see Chow[2]). Let us define the critical slope S_{0c} by

$$S_{0c} = Q^2 n^2 \frac{(2y_c + B)^{4/3}}{(By_c)^{10/3}} > 0,$$

then

$$\begin{array}{rcll} S_0 \leq 0 & \Longrightarrow & \text{ADVERSE SLOPE} & \text{and } y_n = +\infty, \\ 0 < S_0 < S_{0c} & \Longrightarrow & \text{MILD SLOPE} & \text{and } y_n > y_c, \\ S_0 = S_{0c} & \Longrightarrow & \text{CRITICAL SLOPE} & \text{and } y_n = y_c, \\ S & & & \end{array}$$

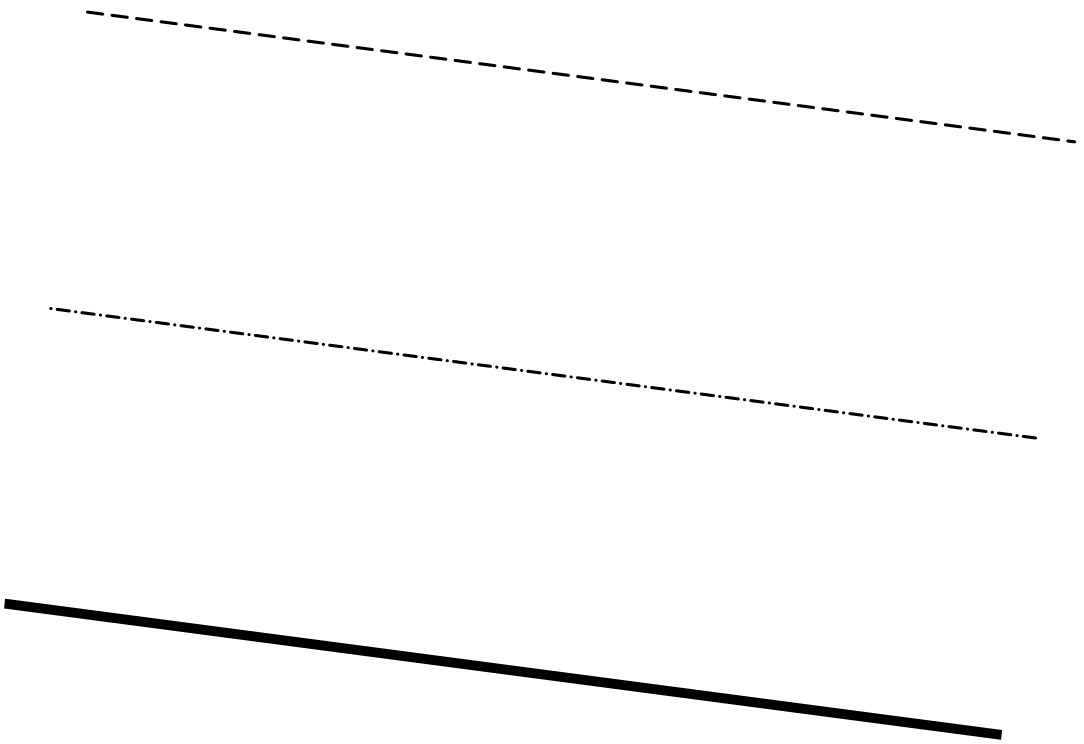

in the previous section, but, since the channel slope now varies with x, the normal depth also varies with x. It is easy to show that the function $y_n(x)$ is bounded, so let $M = \max\{y_n(x) : x \in [0$

3.1 Solution of Discrete Equation

Now that we know that the numerical scheme converges as we refine the grid, we need to think about how we calculate the solution of the numerical scheme. This involves solving a system of $N-1$ nonlinear equations. The most robust method is a pseudo time iteration. Theorem 7 in section 6 gives us the following practical method.

Let $\mathbf{u}^0 = [u_0^0, u_1^0, \ldots, u_N^0]^T > 0$, with $u_0^0 =$

3.2 Po t-Proce ing Solution at Channel End

In certain circumstances when invalid or artificial boundary values γ_0, γ_1 are given to the singular perturbation problem, we find that $Y(0) \neq \gamma_0$ and or $Y(1) \neq \gamma_1$, where Y is the solution of the physical solution of the reduced problem. It is the values of $Y(0)$ and $Y(1)$ that we are interested in. If we let $h \to 0$ we would expect discontinuities in the numerical solution at the boundaries, but a problem arises since we can only solve for finite h, and this results in these discontinuities

4 Results

In this section we include numerical results from five different test problems. For each test problem the analytic solution is known so we can get a good measure of the performance of the numerical scheme. The test problems were created using an "inverse" approach and are published in MacDonald[10]. Full details of the test problems are given in appendix A. The numerical scheme used is that of Engquist-Osher, as described in the previous section, and all the test problems satisfy assumptions (2.19) so all the theory given in the previous two sections is applicable.

For each test problem we show the exact solution, Y, as well as numerical solutions on various grids. The numerical solution is shown by crosses for $N = 10$, triangles for $N = 25$, circles for $N = 50$ and squares for $N = 100$. For each test problem we also show the channel bed profile, the exact free surface profile, and computed free surface profiles.

4.1 Discussion of Results

The solution to test problem 1 is a smooth subcritical flow. Figure 6 shows the exact solution as well as numerical solutions for $N = 10, 25, 50$. The flow for this problem is controlled by the boundary condition at $x = 100$, so it is not surprising that the numerical errors grow as the solution moves away from this boundary. However, they unexpectedly decrease as the solution approaches the other boundary. It can be seen that the numerical solutions give a good approximation to the exact solution and also it can be seen visually that the accuracy increases as the grid is refined. This has been confirmed experimentally by calculating the L_2 errors for a large range of grids and as expected the scheme is found to give a first order accuracy.

The solution to test problem 2 is a smooth supercritical flow. Figure 8 shows the exact solution as well as numerical solutions for $N = 10, 25$. The flow for this problem is controlled by the boundary condition at $x = 0$, and the numerical errors grow as the solution moves away from this boundary; moreover, as in the previous problem they eventually start to decrease. Again it can be seen that the numerical solutions give a good approximation to the exact solution and also the accuracy increases as we refine the grid.

The solution to test problem 3 is a smooth flow that is subcritical for $x \leq 50$ and supercritical for $x \geq 50$. Figure 10 shows the exact solution as well as numerical solutions for $N = 10, 25$. This problem has no boundary conditions; the flow is controlled by the critical section at $x = 50$. This explains why the numerical errors grow as we move away from this point. Again the numerical solutions give a good approximation to the exact solution and the accuracy increases as we refine the grid.

The solution to test problem 4 is a discontinuous flow with a jump at $x = 200/3$. Figure 12 shows the exact solution as well as numerical solutions for $N = 25, 50, 100$. For this problem a boundary condition is given at $x = 100$. The numerical solutions for this rather hard problem are very good. The jump is resolved very well taking into account the coarseness of the grids used. It can be seen visually that both the position and height of the jumps become more

accurate as the grid is refined, but unlike the previous problems with smooth solutions, there are no simple methods to quantitatively confirm this improvement in accuracy. Further refinement beyond that shown here continues the improvement in the numerical solution.

The solution to test problem 5 is also a discontinuous flow and has a jump at $x = 100/3$. Figure 14 shows the exact solution as well as numerical solutions for $N = 10, 25, 50$.

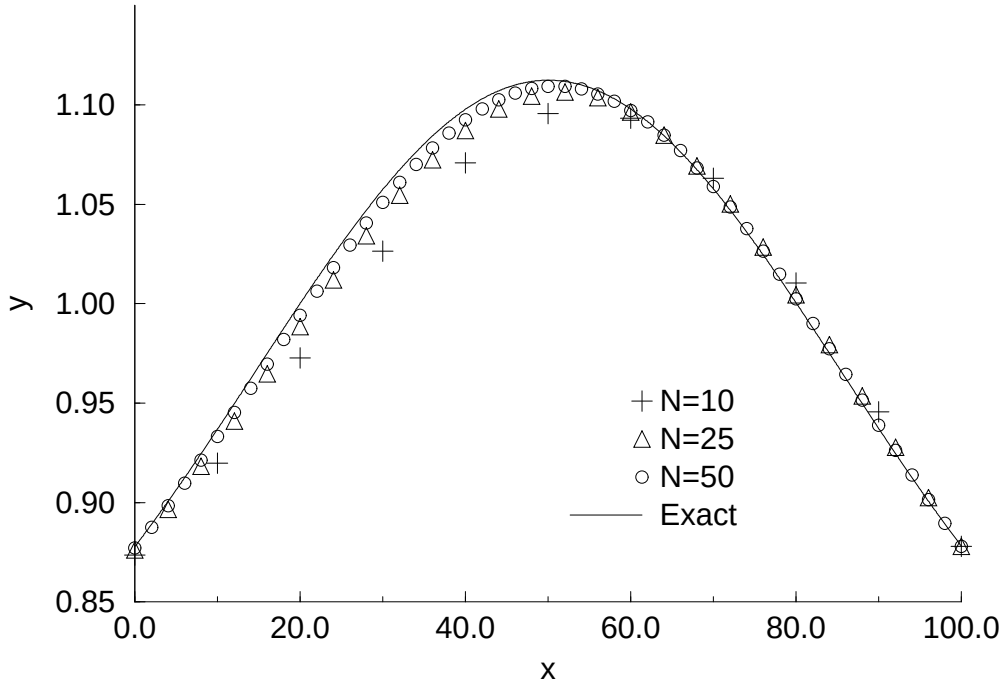

Figure 6: Numerical solutions against exact solution for problem 1

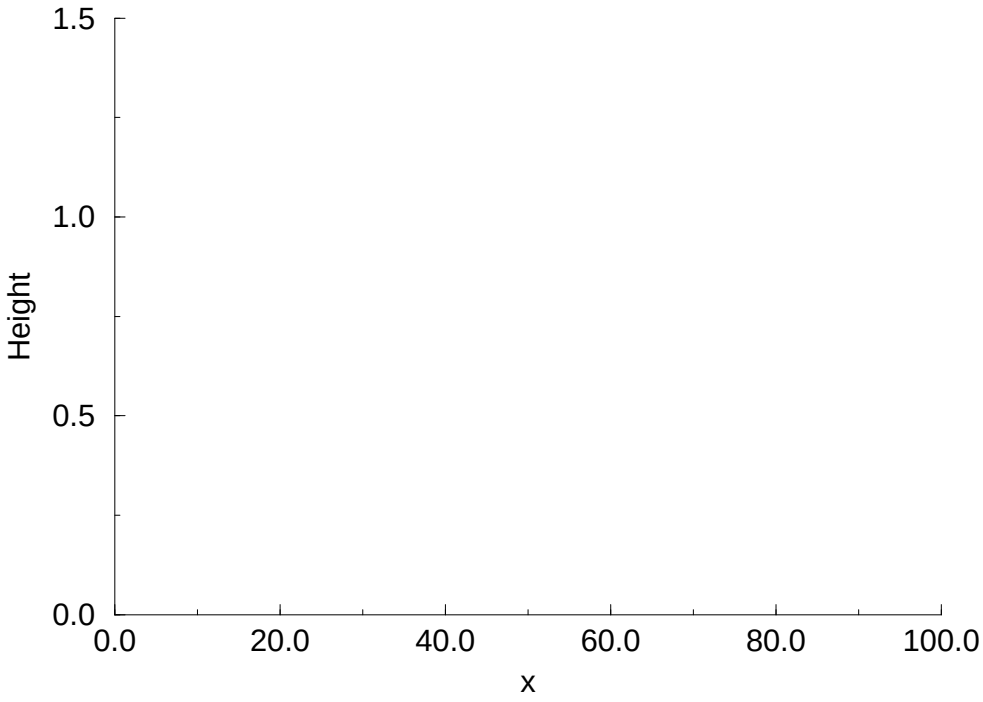

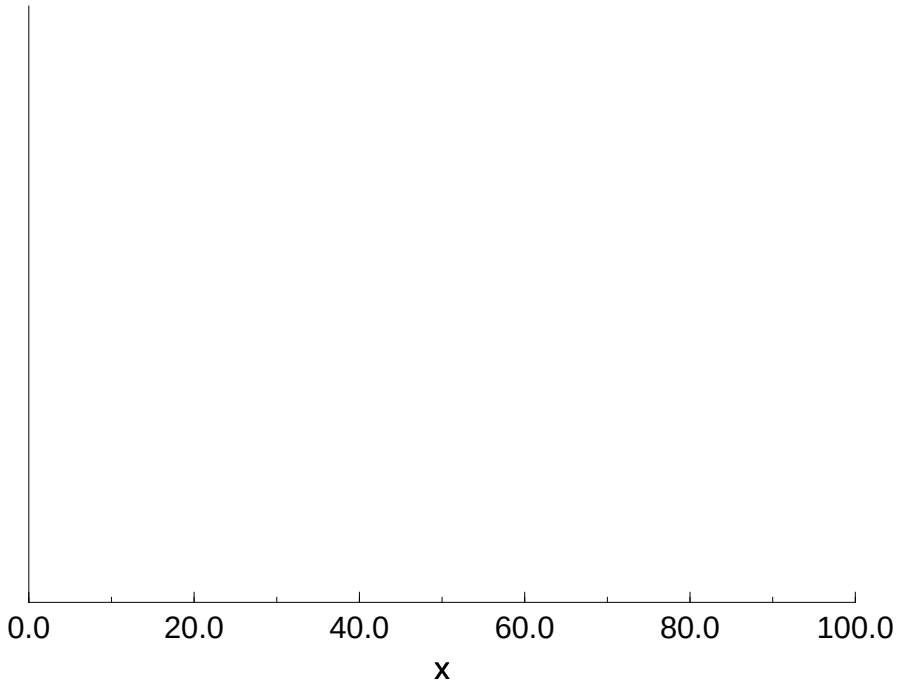
0.0
20.0
40.0
60.0
80.0
100.0
x

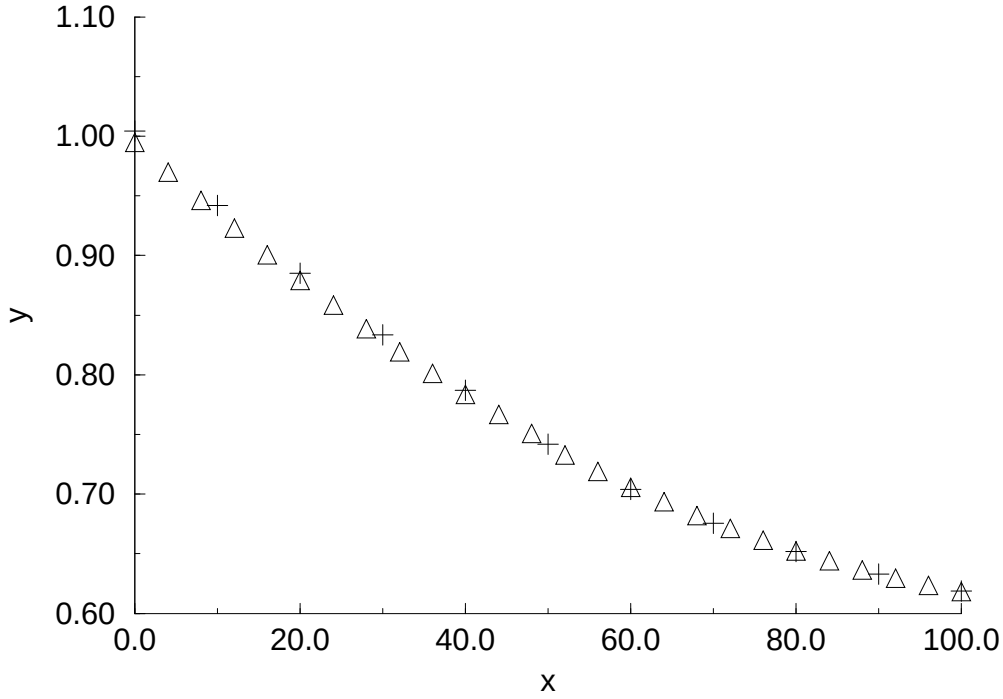
1.10
1.00
0.90
0.80
0.70
0.60
y
0.0
20.0
40.0
60.0
80.0
100.0
x

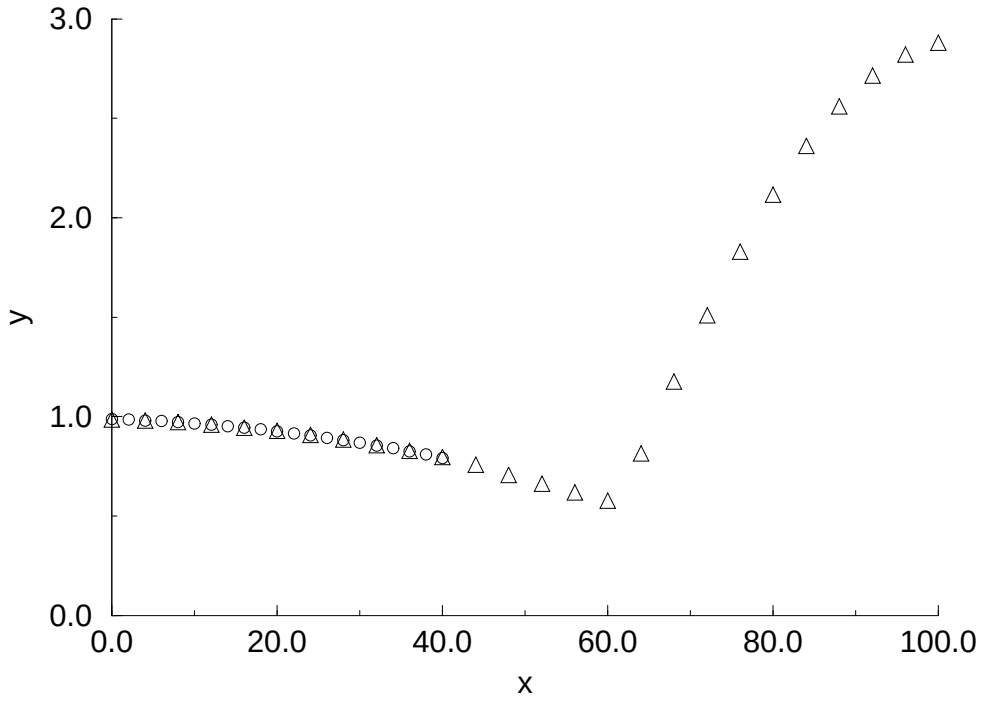
3.0
2.0
1.0
0.0
y
0.0
20.0
40.0
60.0
80.0
100.0
x

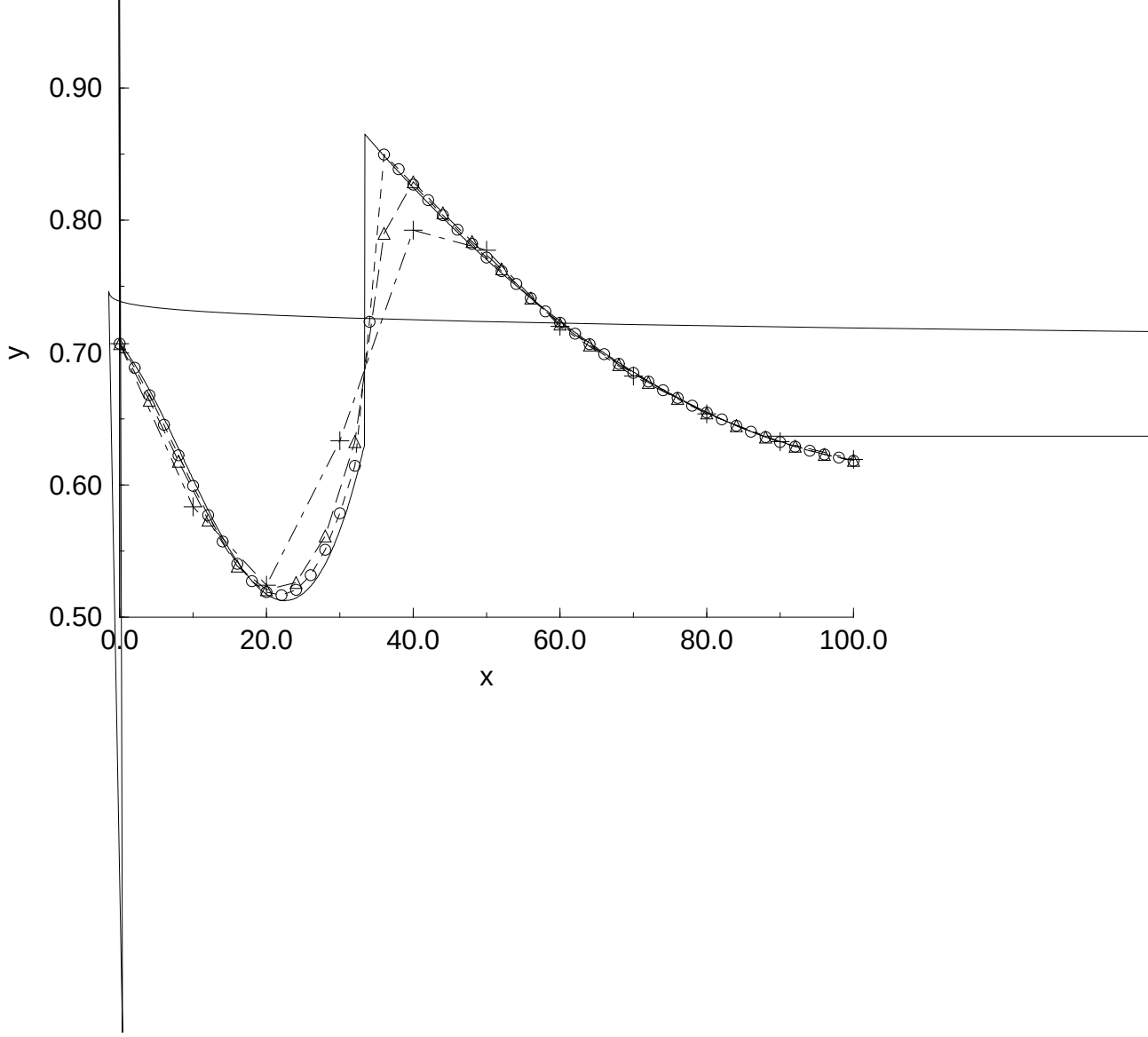
0.90
0.80
0.70
0.60
0.50
y
0.0
20.0
40.0
60.0
80.0
100.0
x

5 Analysis of a Class of Singular Perturbation Problems

In this section we prove a number of results concerning the problem

$$\epsilon \frac{d^2 y_\epsilon}{dx^2} - \frac{d}{dx} f(y_\epsilon) - b(x, y_\epsilon) = 0, \quad y_\epsilon(x) > 0, \quad 0 \le x \le 1, \tag{5.41}$$

$$y_\epsilon(0) = \gamma_0, \quad y_\epsilon(1) = \gamma_1,$$

where ϵ,γ_0,$\gamma_1 > 0$, which are relevant to the steady Saint-Venant problem and have already been used in section 2. Here $b_x, b_y, b_{xy} \in C^0([0,1]\times I\!R_+)$, $f \in C^2(I\!R_+)$ and we have

$$b_y(x, y) > 0, \quad \forall (x, y) \in [0, 1] \times I\!R_+. \tag{5.42}$$

We also assume that there exist m,$M > 0$ such that

$$\begin{array}{rcl} (x, y) \in [0, 1] \times (0, m] & \Longrightarrow & b(x, y) \le 0, \\ (x, y) \in [0, 1] \times [M, \infty) & \Longrightarrow & b(x, y) \ge 0. \end{array} \tag{5.43}$$

We let $\underline{y} = \min\{\gamma_0, \gamma_1, m\}$ and $\overline{y} = \max\{\gamma_0, \gamma_1, M\}$.

This problem without the solution restricted to being positive is well known, for example see Lorenz[8][9]. The existing results do not directly apply to our problem because they require the functions f and b to be defined for all y. We are particularly interested in problems where these functions are singular at $y = 0$. In order to use the existing analysis we construct another problem from (5.41) to which we can apply the existing results. Then, because of the way our new problem has been constructed, we can infer information about the original problem.

The intermediate problem we shall consider is as follows:

$$\epsilon \frac{d^2 \tilde{y}_\epsilon}{dx^2} - \frac{d}{dx} \tilde{f}(\tilde{y}_\epsilon) - \tilde{b}(x, \tilde{y}_\epsilon) = 0, \quad 0 \le x \le 1, \tag{5.44}$$

$$\tilde{y}_\epsilon(0) = \gamma_0, \quad \tilde{y}_\epsilon(1) = \gamma_1.$$

We define the functions $\tilde{f}$ and $\tilde{b}$ by

$$\tilde{f}(y) = \begin{cases} [\frac{1}{2}(f''(\overline{y}) + 2f'(\overline{y}) + f(\overline{y}))(y - \overline{y})^2 & y > \overline{y} \\ +(f'(\overline{y}) + f(\overline{y}))(y - & \\ & \\ & \\ & \\ & \end{cases}$$

Theorem 1 Existence and Uniqueness
Problem (5.41) has a unique solution, $y_\epsilon \in C^2[0,1]$, for all $\epsilon > 0$. This solution satisfies

$$\underline{y} \leq y_\epsilon(x) \leq \overline{y}, \qquad 0 \leq x \leq 1. \tag{5.48}$$

Proof.

Lorenz[8] proves that problem (5.44) has a unique solution, $\tilde{y}_\epsilon \in C^2[0,1]$.

Proof.

Suppose $x \in [0,1)$. Let $r_k = (1-x)/k$ and consider the sequence of intervals given by I

6 Analysis of a Class of Monotone Difference Schemes for the Singular Perturbation Problem

In this section we analyse a family of numerical schemes for solving problem (5.41). We consider a uniform grid $x_i = i/h$, $i = 0, 1, \ldots, N$ and the difference scheme

$$\frac{\epsilon}{h^2}(u_{i+1} - 2u_i + u_{i-1}) - \frac{1}{h}(g(u_{i+1}, u_i) - g(u_i, u_{i-1})) - b(x_i, u_i) = 0, \qquad (6.56)$$

$i = 1, \ldots, N-1$,

$$u_0 = \gamma_0, \qquad u_N = \gamma_1.$$

Here the "numerical flux function" $g(u, v) \in C^0(\mathbb{R}^2_+)$ is subject to consistency and monotonicity conditions

$$g(u, u) = f(u), \qquad (6.57)$$

$$\begin{array}{rcll} u & \rightarrow & g(u, v) & \text{is nonincreasing,} \\ v & \rightarrow & g(u, v) & \text{is nondecreasing.} \end{array} \qquad (6.58)$$

We also require that, for any bounded set $\Omega \subset \mathbb{R}^2_+$, there is a constant $L_\Omega > 0$ such that for all $[u_1, v_1]^T, [u_2, v_2]^T \in \Omega$,

$$|g(u_1, v_1) - g(u_2, v_2)| \leq L_\Omega(|u_1 - u_2| + |v_1 - v_2|). \qquad (6.59)$$

We shall be most interested in the C^1 numerical flux function of Engquist-Osher given by

$$g(u, v) = \int_c^u \min\{f'(s), 0\} ds + \int_c^v \max\{f'(s), 0\} ds, \qquad (6.60)$$

where $c > 0$ is some arbitrary value.

6.1 Exi tence and Uniquene of Di crete Solution

Lemma 2 *Let $\Omega = [y_L, y_R]^2 \subset \mathbb{R}^2_+$. Then for any $u_1, v_1, u_2, v_2 \in [y_L, y_R]$*

$$g(u_1, v_1) - g(u_2, v_2) = (u_1 \; 1 \quad))_{1, u_1} \qquad 1$$

Lemma 3 *Let $0 < y_L \le y_R$, $h > 0$ and $\epsilon \ge 0$. There exists a value $\Delta t^{\epsilon,h}_{y_L,y_R} > 0$ such that, for $0 < \Delta t < \Delta t^{\epsilon,h}_{y_L,y_R}$,*

$$\Delta t \left[\frac{2\epsilon}{h^2} + \frac{1}{h} \left(L^v(s_1, s_2, s_3) - L^u(s_1, s_2, s_4) \right) + b_y(x, s_5) \right] < 1, \tag{6.61}$$

for all $s_1, s_2, s_3, s_4, s_5 \in [y_L, y_R]$, $x \in [0, 1]$.

Proof.

Let

$$\overline{b_y} = \max\{b_y(x, y) : (x, y) \in [0, 1] \times [y_L, y_R]\} > 0. \tag{6.62}$$

Now let

$$\Delta t^{\epsilon,h}_{y_L,y_R} = \left[\frac{2\epsilon}{h^2} + \frac{2}{h} \mathrm{L}_\Omega + \overline{b_y} \right]^{-1},$$

where $\Omega = [y_L, y_R]^2$. It is easily seen that this value satisfies the lemma.

Lemma 4 *Let $0 < y_L \le \underline{y}$, $y_R \ge \overline{y}$, $\epsilon \ge 0$ and $h = 1/N$, where $N - 1 \in \mathbb{N}$. Let us define the set*

$$\Lambda^{N+1}_{y_L,y_R} = \left\{ \mathbf{u} = [u_0, u_1, \ldots, u_N]^T \in \mathbb{R}^{N+1} : u_0 = \gamma_0, u_N = \gamma_1, y_L \le \mathbf{u} \le y_R \right\} \tag{6.63}$$

and the operator $\mathbf{G} : \mathbb{R}^{N+1}_+ \longrightarrow \mathbb{R}^{N+1}$ by

$$\mathbf{G}(\mathbf{u})|_i = \begin{cases} \gamma_0 & i = 0, \\ u_i + \Delta t (T^\epsilon_h \mathbf{u})_i & i = 1, \ldots, N-1, \\ \gamma_1 & i = N, \end{cases} \tag{6.64}$$

where

$$(T^\epsilon_h \mathbf{u})_i = \frac{\epsilon}{h^2} (u_{i+1} - 2u_i + u_{i-1}) - \frac{1}{h} (g(u_{i+1}, u_i) - g(u_i, u_{i-1})) - b(x_i, u_i) \tag{6.65}$$

and $0 < \Delta t < \Delta t^{\epsilon,h}_{y_L,y_R}$. Then we have the following:

(i) $\mathbf{u}, \mathbf{v} \in \mathbb{R}^{N+1}$, $y_L \le \mathbf{u} \le \mathbf{v} \le y_R \Longrightarrow \mathbf{G}(\mathbf{u}) \le \mathbf{G}(\mathbf{v})$.

(ii) $\mathbf{G}(\Lambda^{N+1}_{y_L,y_R}) \subset \Lambda^{N+1}_{y_L,y_R}$.

(iii) $\mathbf{u}, \mathbf{v} \in \Lambda^{N+1}_{y_L,y_R} \Longrightarrow \| \mathbf{G}(\mathbf{u}) - \mathbf{G}(\mathbf{v}) \|_1 \le (1 - \Delta t \delta_{y_L,y_R}) \| \mathbf{u} - \mathbf{v} \|_1$,

where

$$\delta_{y_L,y_R} = \min\{b_y(x, y) : (x, y) \in [0, 1] \times [y_L, y_R]\}. \tag{6.66}$$

Note that $0 < 1 - \Delta t \delta_{y_L,y_R} < 1$.

Proof.

(i). Let $\mathbf{u}, \mathbf{v} \in \mathbb{R}^{N+1}$, with $y_L \le \mathbf{u} \le \mathbf{v} \le y_R$. Now for $1 \le i \le N - 1$

$$\mathbf{G}(\mathbf{v})|_i - \mathbf{G}_h(\mathbf{u})|_i = w_i + \frac{\epsilon \Delta t}{h^2} (w_{i+1} - 2w_i + w_{i-1})$$

$$- \frac{\Delta t}{h} (g(v_{i+1}, v_i) - g(u_{i+1}, u_i)) + \frac{\Delta t}{h} (g(v_i, v_{i-1}) - g(u_i, u_{i-1}))$$

$$-\Delta t(b(x, v_i) - b(x, u_i)),$$

where $w_i = v_i - u_i$

$$+|w_0|\Delta t\left[\frac{\epsilon}{h^2}+\frac{1}{h}L^v(v_0,u_0,u_1)\right]+|w_N|\Delta t\left[\frac{\epsilon}{h^2}-\frac{1}{h}L^u(v_N,u_N,v_{N-1})\right]$$

$$-|w_1|\Delta t\left[\frac{\epsilon}{h^2}-\right.$$

L

6.2 Convergence a $h,\epsilon \to 0$

In section 5 we proved the existence of a unique physical solution, $Y \in NBV$, of the reduced problem ($\epsilon \to 0$). We now give a theorem that shows that, if we apply the above numerical scheme then, as $\epsilon \to 0$, the numerical solution is guaranteed to converge to Y.

Theorem 8 *Let $\mathbf{u}_h^0 = [u_0^{0,h}, u_1^{0,h}, \ldots, u_N^{0,h}]^T$ denote the discrete solution of (6.56) for $\epsilon = 0$ and let U^h be the piecewise constant function*

$$U^h(x) = u_i^{0,h} \text{ for } ih \le x \le ih + h,\ i = 0, 1, \ldots N-1. \tag{6.71}$$

Let $\{h_n\}$ be a null sequence where each $h_n = 1/(j+1)$ for some $j \in \mathbb{N}$, then there is a subsequence $\{h_{n_k}\}$ such that

$$U^{h_{n_k}} \to Y \in NBV \quad a.e.\ as\ k \to \infty. \tag{6.72}$$

Y is the unique function in NBV that satisfies conditions (i),(ii) and (iii) in theorem 3.

Proof.

To prove this result we take the same approach as in the analysis in section 5. We look at the numerical scheme

$$\frac{\epsilon}{h^2}(u_{i+1} - 2u_i + u_{i-1}) - \frac{1}{h}(\tilde{g}(u_{i+1}, u_i) - \tilde{g}(u_i, u_{i-1})) - \tilde{b}(x_i, u_i) = 0, \tag{6.73}$$

$i = 1, \ldots, N-1$,

$$u_0 = \gamma_0, \quad u_N = \gamma_1,$$

for solving problem (5.44). Here $\tilde{g}$ is given by

$$\tilde{g}(u,v) = \begin{cases} g(u,v) & \underline{y} \le u \le \overline{y} \text{ and } \underline{y} \le v \le \overline{y}, \\ g(\overline{y},\overline{y}) + H_1(u;\overline{y}) + H_2(v;\overline{y}) & u > \overline{y} \text{ and } v > \overline{y}, \\ g(\overline{y},v) + H_1(u;\overline{y}) & u > \overline{y} \text{ and } \underline{y} \le v \le \overline{y}, \\ g(\overline{y},\underline{y}) + H_1(u;\overline{y}) + H_2(v;\underline{y}) & u > \overline{y} \text{ and } v < \underline{y}, \\ g(u,\underline{y}) + H_2(v;\underline{y}) & \underline{y} \le u \le \overline{y} \text{ and } v < \underline{y}, \\ g(\underline{y},\underline{y}) + H_1(u;\underline{y}) + H_2(v;\underline{y}) & u < \underline{y} \text{ and } v < \underline{y}, \\ g(\underline{y},v) + H_1(u;\underline{y}) & u < \underline{y} \text{ and } \underline{y} \le v \le \overline{y}, \\ g(\underline{y},\overline{y}) + H_1(u;\underline{y}) + H_2(v;\overline{y}) & u < \underline{y} \text{ and } v > \overline{y}, \\ g(u,\overline{y}) + H_2(v;\overline{y}) & \underline{y} \le u \le \overline{y} \text{ and } v > \overline{y}, \end{cases} \tag{6.74}$$

where

$$H_1(u;z) = \int_z^u \min\{\tilde{f}'(s)\}ds, \tag{6.75}$$

and

$$H_2(v;z) = \int_z^v \max\{\tilde{f}'(s)\}ds. \tag{6.76}$$

Since $H_1(z;z) = 0$ and $H_2(z;z$

the fact that H_1, H_2 have bounded deriv

7 Conclusions and Further Work

For a rectangular channel with positive bed slope, we have shown that the unique physical steady flow can be obtained as the zero viscosity limit of solutions to a sequence of viscous problems which are generated by adding an artificial viscosity term, of strength ϵ, to the steady Saint-Venant equations. By this limiting process we also obtained a family of numerical schemes which are guaranteed to converge to the physical solution in the limit as the grid size tends to zero. We demonstrated that these schemes are well behaved in the sense that the numerical solution always exists and is uniformly bounded. We have also given numerical results for a particular member of this class of schemes for a series of test problems. The results show that the numerical scheme approximates the solution well in smooth regions and also gives very good resolution of the discontinuities.

In the future we would like to extend the theory given in this report to a less restrictive class of channels. The extension of the analysis to certain other shapes orkv

References

[1] U M Asc

[16] Karl R Stromberg. *An Introduction to Classical Real Analysis*. Wadsworth International, Belmont, California, 1981.

A Notation

$\mathbb{R}_+$	$(0, \infty)$
$\mathbf{u}$	Bold denotes a vector
$\mathbf{u}\,\vert_i$	i'th component of vector
$\mathbf{u} \leq \alpha$	$\mathbf{u}\,\vert_i \leq \alpha$ for all i; same for $=$, $\geq$, $<$ and $>$
$\mathbf{u} \leq \mathbf{v}$	$\mathbf{u}\,\vert_i \leq \mathbf{v}\,\vert_i$ for all i; same for $=$, $\geq$, $<$ and $>$
$\mathrm{sg}(z)$	$\mathrm{sg}(z) = -1, 0, 1$ for $z < 0, = 0, > 0$
$C^n(A)$	Set of functions $f : A \longrightarrow \mathbb{R}$ that have n continuous derivatives
$u(x+)$	Limit $u(x + \delta)$, as $\delta \to 0$ from above
$u(x-)$	Limit $u(x - \delta)$, as $\delta \to 0$ from above
BV	Functions of Bounded Variation on $[0, 1]$
NBV	$\{u \in BV : u(x) = u(x+),\ \text{for } x \in [0, 1), u(1) = u(1-)\}$
$C_0^\infty(0, 1)$	Smooth test functions with compact support on $(0, 1)$
$\|\mathbf{u}^h\|_1$	$h \sum_{i=0}^{N} \|u_i\|$

B Details of Test Problems

In this Appendix we give details of the test problems used in section 4. The exact solutions are illustrated in figures 6-15.

Problem 1 ***Subcritical Flow***

A rectangular channel, $0 \leq x \leq 100m$, has width $10m$ and a discharge of $20m^3s^{-1}$. The slope of the channel is given by

$$S_0(x) = \left(1 - \frac{4}{g[\hat{y}(x)]^3}\right)\hat{y}'(x) + \frac{9}{2500[\hat{y}(x)]^2}\left(\frac{1}{5} + \frac{1}{\hat{y}(x)}\right)^{4/3},$$

where

$$\hat{y}(x) = \left(\frac{4}{g}\right)^{1/3}\left(1 + \frac{1}{2}\exp\left[-4\left(\frac{x}{100} - \frac{1}{2}\right)^2\right]\right),$$

and

$$\hat{y}'(x) = -\left(\frac{4}{g}\right)^{1/3}\frac{1}{25}\left(\frac{x}{100} - \frac{1}{2}\right)\exp\left[-4\left(\frac{x}{100} - \frac{1}{2}\right)^2\right].$$

Manning's friction coefficient for the channel is 0.03. The flow is subcritical at outflow, with depth $\hat{y}(100)$, and subcritical at inflow.

The exact solution for this problem is $y(x) \equiv \hat{y}(x)$.

Problem 2 ***Supercritical Flow***

A rectangular channel, $0 \leq x \leq 100m$, has width $10m$ and a discharge of $20m^3s^{-1}$. The slope of the channel is given by

$$S_0(x) = \left(1 - \frac{4}{g[\hat{y}(x)]^3}\right)\hat{y}'(x) + \frac{9}{2500[\hat{y}(x)]^2}\left(\frac{1}{5} + \frac{1}{\hat{y}(x)}\right)^{4/3},$$

where

$$\hat{y}(x) = \left(\frac{4}{g}\right)^{1/3}\left(1 - \frac{1}{4}\exp\left[-4\left(\frac{x}{100} - \frac{1}{2}\right)^2\right]\right),$$

and

$$\hat{y}'(x) = \left(\frac{4}{g}\right)^{1/3}\frac{1}{50}\left(\frac{x}{100} - \frac{1}{2}\right)\exp\left[-4\left(\frac{x}{100} - \frac{1}{2}\right)^2\right].$$

Manning's friction coefficient for the channel is 0.03. The flow is supercritical at inflow, with depth $\hat{y}(0)$ and supercritical at outflow.

The exact solution for this problem is $y(x) \equiv \hat{y}(x)$.

Problem 3 ***Transcritical Flow***

A rectangular channel, $0 \leq x \leq 100m$, has width $10m$ and a discharge of $20m^3s^{-1}$. The slope of the channel is given by

$$S_0(x) = \left(1 - \frac{4}{g[\hat{y}(x)]^3}\right)\hat{y}'(x) + \frac{9}{2500[\hat{y}(x)]^2}\left(\frac{1}{5} + \frac{1}{\hat{y}(x)}\right)^{4/3},$$

where

$$\hat{y}(x) = \left(\frac{4}{g}\right)^{1/3}\left(1 - \frac{(x-50)}{200} + \frac{(x-50)^2}{30000}\right),$$

and

$$\hat{y}'(x) = \left(\frac{4}{g}\right)^{1/3}\left(-\frac{1}{200}\right.$$

and

$$\hat{y}'(x) = \begin{cases} \left(\frac{4}{g}\right)^{1/3}\left(-0.431488\left(\frac{x}{100}-\frac{1}{3}\right)^3 + 0.566331\left(\frac{x}{100}-\frac{1}{3}\right)^2 \right. & x \le \frac{100}{3} \\ \left. +0.358658\left(\frac{x}{100}-\frac{1}{3}\right) + 0.031725\right) & \\ & \\ \frac{-1}{200}\left(\frac{4}{g}\right)^{1/3} + \frac{4}{500}\left(\frac{x}{100}-\frac{2}{3}\right) & x > \frac{100}{3} \end{cases}.$$

Manning's friction coefficient for the channel is 0.03. The flow is supercritical at inflow, with depth $\hat{y}(0)$ and supercritical at outflow.

The exact solution for this problem is $y(x) \equiv \hat{y}(x)$.